THE g-FACTOR OF THE BOUND ELECTRON: A TEST OF BOUND-STATE QED*

K. HERMANSPAHN[a], W. QUINT[b], S. STAHL[a], M. TÖNGES[a],

G. BOLLEN[b], H.-J. KLUGE[b], R. LEY[a], R. MANN[b] AND G. WERTH[a]

[a] Johannes-Gutenberg-Universität, Mainz, Germany
[b] GSI Darmstadt, Germany

(Received December 8, 1995)

The measurement of the electronic g-factor of hydrogenic ions is a sensitive test of bound-state QED (Quantum Electrodynamics). The deviations of the g-factor of the bound electron from the free-electron value are mainly due to i) the relativistic binding energy correction $-(Z\alpha)^2/3$ and ii) the bound-state radiative correction $\alpha(Z\alpha)^2/4\pi$. In the experiment a single hydrogenic ion is stored in the magnetic field of a Penning trap. The g-factor is measured by inducing spin-flip transitions with a microwave field. The magnetic field is calibrated measuring the cyclotron frequency of the stored ion. In the Penning trap the ion is detected electronically and cooled to 4° K through a superconducting resonance circuit connected to the trap electrodes.

PACS numbers: 12.20.Fv, 31.30.Jv, 32.30.Bv

1. Introduction: bound-state QED

The g-factor of the electron relates its magnetic moment μ, in units of the Bohr magneton μ_B, to its spin angular momentum s, in units of Planck's constant $\hbar$.

$$\frac{|\mu|}{\mu_B} = g\frac{|s|}{\hbar}. \tag{1}$$

In the Dirac theory the g-factor of the free electron is

$$g_{\text{Dirac}} = 2. \tag{2}$$

* Presented at the XXIV Mazurian Lakes School of Physics, Piaski, Poland, August 23–September 2, 1995.

The g-factor of the electron differs slightly from the Dirac value because the electron interacts with the radiation field *(radiative corrections)*. The different contributions to the g-factor of the electron can be grouped into the following categories (electron-electron interactions are not discussed here because we focus on one-electron systems):

I. the relativistic binding energy correction (Breit term);
II. the radiative corrections of the free electron;
III. the radiative corrections in the bound state;
IV. the nuclear corrections due to the finite mass, the finite size and the polarization

of the nucleus.

I. The relativistic binding correction:

The g-factor of the electron in the Coulomb field of a nucleus with charge Ze was first calculated by Breit in 1928 who solved the Dirac equation for the bound system [1]. The modification to the g-factor of the electron in the bound state (compared to the free electron) depends on its mean kinetic energy [2] and thus on its binding energy, *i.e.* the Dirac energy E_{Dirac} of the $1s_{1/2}$ state, given by

$$E_{\text{Dirac}} = m_e c^2 \sqrt{1 - (Z\alpha)^2}\,. \tag{3}$$

According to Breit [1] the g-factor is reduced in the bound state by

$$\frac{g_{\text{Breit}}}{2} = \tfrac{1}{3}\left(1 + 2\sqrt{1 - (Z\alpha)^2}\right) = 1 - \tfrac{1}{3}(Z\alpha)^2 - \tfrac{1}{12}(Z\alpha)^4 + 0(Z\alpha)^6. \tag{4}$$

II. Radiative corrections:

The first calculation of a radiative correction to the g-factor of the free electron was done by Schwinger. The Schwinger term α/π describes the virtual emission and absorption of a photon by the electron. The higher-order terms account for the virtual emission and absorption of several photons and for the vacuum polarization. Meanwhile, the radiative corrections were calculated up to the eighth order ($\propto \alpha^4$) [3]

$$\frac{g_{\text{free}}}{2} = 1 + C_1\left(\frac{\alpha}{\pi}\right) + C_2\left(\frac{\alpha}{\pi}\right)^2 + C_3\left(\frac{\alpha}{\pi}\right)^3 + C_4\left(\frac{\alpha}{\pi}\right)^4 + 0\left(\frac{\alpha}{\pi}\right)^5. \tag{5}$$

The precision of these calculations is limited by our knowledge of the fine structure constant α. The theoretical prediction is experimentally confirmed to a level of $\delta g_e/g_e = 10^{-11}$ [4].

III. Bound-state radiative corrections:

In addition to the radiative corrections of the free electron, the g-factor of the bound electron in the $1s_{1/2}$ state is modified by bound-state radiative corrections [5].

$$\frac{g(1s)}{g_{\rm free}} = 1 - \tfrac{1}{3}(Z\alpha)^2 + \frac{\alpha}{4\pi}(Z\alpha)^2. \qquad (6)$$

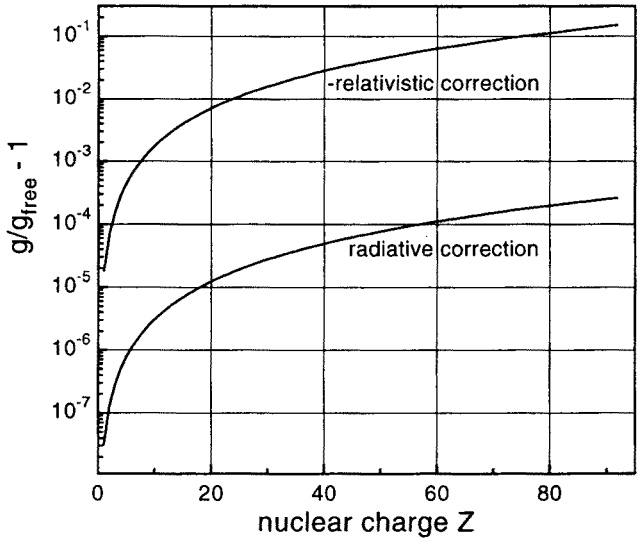

Fig. 1. Deviation of the g-factor of the bound electron from the free-electron value due to the relativistic Breit correction $-\frac{1}{3}(Z\alpha)^2$ (upper curve) and the radiative bound-state QED correction $+\frac{\alpha}{4\pi}(Z\alpha)^2$ (lower curve) as a function of the nuclear charge Z.

The leading bound-state correction is the Breit term $-(1/3)(Z\alpha)^2$ (see Eq. (4) and Fig. 1). Note that in (6) the term of the order $(Z\alpha)^4$ from Eq. (4) is omitted. For heavy ions, however, this term cannot be neglected. The term $(\alpha/4\pi)(Z\alpha)^2$ is the lowest order bound-state radiative correction. Calculations of the higher-order radiative corrections are not available, but are underway [6]. Possibly, the g-factor calculations have to be treated numerically for high-Z systems, just as in the case of the Lamb shift calculations. The experimental determination of the g-factor of the bound electron in hydrogenic systems is a precision test of the magnetic sector of QED in

the strong Coulomb field of the nucleus. The theoretical methods for the calculations of the g-factor of the bound electron are similar to those of the M1-transitions between the hyperfine levels of the 1s ground state in hydrogenic heavy ions, which have been investigated with laser spectroscopy [7]. The g-factor of the bound electron, however, is less sensitive to the details of the nuclear structure, since the nucleus influences the g-factor only via the dependence of the electronic wave function on the nuclear properties.

IV. Nuclear corrections:

In the formulas (4) and (6) the motion of the nucleus is neglected, *i.e.* it is assumed that the nucleus has an infinite mass. The correction terms due to the finite mass of the nucleus have to be added to (6) [5]

$$\begin{aligned}\frac{g(1s)}{g_{\text{free}}} &= 1 - \frac{1}{3}(Z\alpha)^2 + \frac{\alpha}{4\pi}(Z\alpha)^2 \\ &+ \frac{1}{3}(Z\alpha)^2\left(\frac{3}{2}\frac{m_e}{M_n} - (1+Z)\frac{3}{2}\frac{m_e^2}{M_n^2}\right) \\ &- \frac{\alpha}{4\pi}(Z\alpha)^2\left(\frac{5}{3}\frac{m_e}{M_n} - \frac{6+Z}{3}\frac{m_e^2}{M_n^2}\right). \end{aligned} \tag{7}$$

Here, M_n is the mass of the nucleus. Also the finite size of the nucleus influences the g-factor of the bound electron because it modifies the Breit term. To give an example, the finite size effect is of the order of 10^{-9} in the case of the hydrogenic neon ion (Ne^{9+}) [8], where $g(1s)/g_{\text{free}} - 1 = -2\,10^{-3}$. Another nuclear effect is the nuclear polarization, *i.e.* the virtual excitation of nuclear energy levels. So far, the influence of this effect on the g-factor has not been calculated.

2. Experimental tests: atomic Hydrogen and the Helium ion

The calculations of the g-factor of hydrogenic systems were tested in only very few experiments. The nuclear mass correction (Eq. (7)) was verified in a comparison of the g-factors of the hydrogen and the deuterium atom in a hydrogen maser with an accuracy of $4\,10^{-3}$ [9]. With the technique of spin-exchange optical pumping the g-factor of atomic hydrogen was compared to the g-factor of the free electron confirming the relativistic Breit term $-(1/3)(Z\alpha)^2$ with an accuracy of $7\,10^{-4}$ and the bound-state radiative correction $(\alpha/4\pi)(Z\alpha)^2$ with an accuracy of about 40 percent [10]. The first and only measurement of the g-factor of a hydrogenic ion was performed on the helium ion ($^4He^+$). This measurement tested the Breit term $-(1/3)(Z\alpha)^2$ with an accuracy of $5\,10^{-3}$, but was not sensitive to the bound-state radiative correction $(\alpha/4\pi)(Z\alpha)^2$ [11].

3. The Penning trap

3.1. The principles of the Penning trap

In the Penning trap charged particles are stored in a combination of a homogeneous magnetic field and an electrostatic quadrupole field [4, 12]. The magnetic field confines the particles perpendicular to the magnetic field lines, and the electrostatic potential parallel to the magnetic field lines. The three characteristic motions of the particles in the trap are (see Table I):

- the *cyclotron motion* with frequency ω_+, slightly modified by the presence of the electrostatic field,
- the oscillation in the electrostatic potential parallel to the magnetic field lines (*axial motion*) with frequency ω_z and
- the $E \times B$ — drift motion perpendicular to the magnetic field lines (*magnetron motion*) with frequency ω_-.

The free-space cyclotron frequency $\omega_c^{\text{ion}} = q_{\text{ion}}B/M_{\text{ion}}$ (q_{ion} and M_{ion}: charge and mass of the ion) is calculated from the three characteristic frequencies by

$$\omega_c^{\text{ion}} = \sqrt{\omega_+^2 + \omega_z^2 + \omega_-^2}\,. \tag{8}$$

The characteristic frequencies ω_+, ω_z and ω_- are measured very precisely using high-Q resonant circuits, which are connected to the trap electrodes, and a FFT-analyser (Fast-Fourier-Transform). The trapped particles are in thermal contact with the resonant circuits through the image currents induced in the trap electrodes. In this way the particles are cooled to the ambient temperature of 4 Kelvin (*resistive cooling*). For high-precision experiments the cooling of the trapped ions to low temperatures is of great importance to minimize the line broadening due to inhomogeneities of the magnetic field.

3.2. The spin precession frequency

For the determination of the g-factor also the it spin precession frequency ω_s of the bound electron has to be measured.

$$\omega_s = g\frac{\mu_B B}{\hbar} = g\frac{eB}{2\pi m_e}\,. \tag{9}$$

Once the spin precession frequency ω_s and the cyclotron frequency ω_c^{ion} are measured, the g-factor of the hydrogenic ion can be calculated by

$$g = 2\frac{\omega_s}{\omega_c^{\text{ion}}}\frac{m_e}{M_{\text{ion}}}\,. \tag{10}$$

A systematic error at the level of 10^{-9} arises because the mass ratio m_e/M_{ion} has to be taken from the literature. Alternatively, the measurement of the cyclotron frequency of trapped electrons could be used to calibrate the magnetic field.

Several methods exist to measure the g-factor of hydrogenic ions. The measurements on atomic hydrogen and the helium ion (see Section 2) were performed with the particles contained in a gas cell in a magnetic field of about 0.01 Tesla. The polarization of the electronic spins was produced and detected via spin-exchange collisions with optically pumped cesium or rubidium atoms. orientation However, for hydrogenic ions heavier than helium the process of electron capture dominates over the process of spin exchange. Therefore, this method is not applicable to ions heavier than helium.

Another way to measure the g-factor is the *quantum-jump method*, developed by Dehmelt in his g-2 experiment [4]. Here, a single particle is stored in the Penning trap, and its spin precession frequency is measured by inducing quantum jumps between the two possible spin orientations in the strong magnetic field of the Penning trap. In the "ideal" Penning trap the eigenfrequencies ω_+, ω_z and ω_- are independent of the spin orientation. To make the quantum jumps observable, the particle's axial oscillation frequency is coupled to the spin orientation through an additional inhomogeneous magnetic field component $B_2 z^2$ superimposed to the homogeneous field B_0 of the "ideal" Penning trap.

$$B(z) = B_0 + B_2 z^2 \,. \tag{11}$$

Due to the interaction of the magnetic moment of the trapped particle with the magnetic bottle $B_2 z^2$, the axial oscillation frequency depends now on the spin orientation. The change of the axial frequency due to a spin-flip transition is proportional to the strength of the magnetic bottle (see Fig. 2).

$$(\Delta\omega_z)_{\text{spin flip}} = \frac{g\mu_B B_2}{\omega_z M_{\text{ion}}} \,. \tag{12}$$

Experimentally, frequency jumps of a few hundred millihertz can be detected with a single trapped particle (see Table 1).

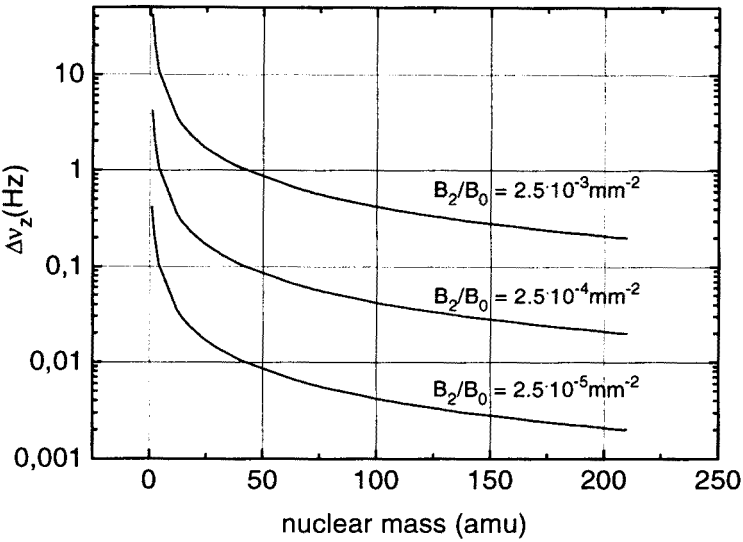

Fig. 2. The axial frequency shift due to a spin-flip transition as a function of the mass of the ion for different magnetic bottles B_2/B_0.

TABLE I

The g-factors and the oscillation frequencies of the hydrogenic ions C^{5+}, Ne^{9+} and U^{91+}. The following parameters are assumed: magnetic field $B_0 = 6$ Tesla, axial frequency shift due to spin flip $\Delta\omega_z/2\pi = 0.2$ Hz, trapping potential $V_0 = 0.5$ Volt and inner diameter of trap electrodes 15 mm.

hydrogenic ion	C^{5+}	Ne^{9+}	U^{91+}
$g/g_{free} - 1$	$-6\cdot10^{-4}$	$-2\cdot10^{-3}$	$-1.5\cdot10^{-1}$
spin precession frequency $\omega_s/2\pi$	168.2 GHz	167.9 GHz	142.9 GHz
cyclotron frequency $\omega_c/2\pi$	38.0 MHz	41.0 MHz	35.0 MHz
axial frequency $\omega_z/2\pi$	100.0 kHz	100.0 kHz	100.0 kHz
magnetron frequency $\omega_-/2\pi$	130.0 Hz	120.0 Hz	140.0 Hz
magnetic bottle B_2/B_0	$1.4\cdot10^{-4}/mm^2$	$2.2\cdot10^{-4}/mm^2$	$2.6\cdot10^{-3}/mm^2$

The spin precession frequency is determined in the following procedure. The axial oscillation frequency of a single trapped hydrogenic ion is continuously measured via the image currents induced in the trap electrodes.

At the same time, spin flips are induced by a microwave field. A change of the axial oscillation frequency indicates the spin-flip transition. At different microwave frequencies the spin-flip rate is measured counting the number of spin-flips in a fixed time interval. When the microwave is in resonance with the spin precession frequency, the spin-flip rate reaches a maximum. For the calibration of the magnetic field, the cyclotron frequency of the ion is measured with the image current method. Finally, after the measurement of the spin precession frequency and the cyclotron frequency, the g-factor of the bound electron is calculated using formula (10). The described method is universal in the sense that it can, in principle, be applied to ions with any charge-to-mass ratio.

3.3. The expected precision

The magnetic bottle $B_2 z^2$, required for the detection of the spin-flip transition, is at the same time the main limitation to the accuracy of the measurement. Because of the quadratic term the averaged magnetic field "seen" by the trapped ion depends on its axial oscillation amplitude z, resulting in a shift of the cyclotron and the spin precession frequency.

$$\frac{\Delta\omega_s}{\omega_s} = \frac{\Delta\omega_c}{\omega_c} = \frac{B_2}{B_0}\frac{E_z}{M_{\text{ion}}\omega_z^2}. \tag{13}$$

Here, $E_z = (1/2)M_{\text{ion}}\omega_z^2 z^2$ is the kinetic energy of the ion in the axial direction. Because of thermal fluctuations of the oscillation amplitude of the ion, the cyclotron frequency as well as the spin precession frequency are broadened. At a temperature of 4 Kelvin the fractional linewidth is less than 10^{-6}. Assuming that the line can be split to 10 %, the expected measurement uncertainty is 10^{-7}. With this accuracy the higher-order radiative corrections to the magnetic moment of the bound electron can be tested on the percent level.

4. The experimental set-up

The trap apparatus is suspended in the vertical bore of a 6 Tesla superconducting magnet. The trap is mounted in a completely sealed vacuum enclosure in order to obtain the ultra-high vacuum necessary for long storage times of the trapped ions. The vacuum enclosure of the trap is thermally connected to a helium dewar at 4° K and cryopumped to an extremely low pressure [13]. A typical liquid helium consumption rate is 1 liter per day for the trap apparatus and 0.5 liter per day for the superconducting magnet. To minimize the radiative heat load of the cryogenic system the magnet bore can be cooled to 77° K with liquid nitrogen, and a radiation

shield (at 20° K) is placed between the trap apparatus and the bore of the superconducting magnet.

The cylindrical trap electrodes are constructed out of OFHC copper and spaced by sapphire rings. The trap electrodes are electrically connected to *i)* dc power supplies to generate the electrostatic trapping potential, *ii)* function generators to excite the energy of the trapped ions and *iii)* the tuned resonant circuits for detection and resistive cooling. In order to minimize the electronic noise, the resonant circuits are kept at a temperature of 4° K. To optimize the sensitivity of the electronic detection system, a high quality factor of the tuned circuits is necessary. Therefore, the resonant circuit for the detection of the axial oscillation frequency is made out of superconducting material (NbTi). The signal from the resonant circuits is amplified, mixed down with a function generator and analysed with a FFT-analyser. The magnetic bottle $B_2 z^2$ is produced by a thin nickel ring placed close to the trap electrodes. The microwave at 160 GHz for the spin-flip transition reaches the cryogenic region through a waveguide and enters the vacuum enclosure through a glass window.

5. The production of hydrogenic ions

There are several different techniques to produce highly charged ions:

- *electron impact ionization*
- *recoil ions* and
- *stripping of fast ion beams in target foils.*

With the method of *electron impact ionization* highly charged ions are produced in a step-by-step process through multiple collisions with electrons. This scheme is well-known from the electron beam ion sources (EBIS) where the ions are trapped longitudinally by an electrostatic potential and radially by a magnetic field and the space-charge potential of an electron beam [14]. The production rate of fully stripped ions depends strongly on the nuclear charge Z, because the ionization potential of a given shell scales as Z^2 and the ionization cross section roughly as Z^{-4} [15]. Therefore, both the energy and the density of the electron beam, necessary to strip the ions, increase with Z. Calculations of production rates for different values of Z are available [14]. Here only one example may be given: a sample of neutral neon atoms (^{20}Ne) is fully stripped within 10 seconds in an electron beam with a current of 50 mA, a beam diameter of 1 mm and an energy of 5 keV. With this method fully stripped uranium ions U^{92+} have been produced recently [16].

Highly charged ions can also be produced as *recoil ions* in collisions of a fast (MeV) ion beam with a thermal atomic or molecular gas target [17].

The heavy-ion projectile can remove a large number of electrons from the target atom in a single collision without transferring much kinetic energy to the recoil ion (only a few eV). At such low kinetic energies the ions can be loaded directly into an ion trap. This multiple ionization process involves different mechanisms like Coulomb ionization, electron transfer to the projectile and autoionization. The cross section for the production of fully stripped ions depends in a complicated way on the collision parameters and decreases rapidly with Z.

Highly charged ions up to bare uranium can be produced by stripping a high-energy ion beam in a thin target foil. In the ESR (Experimental Storage Ring) at GSI about 10^8 bare uranium ions (U^{92+}) can be injected at energies of a few hundred MeV/u, stored, electron cooled and decelerated to presently 50 MeV/u. In order to trap the highly charged ions in an ion trap, it would be necessary to extract the ions in short bunches from the ESR, to further decelerate them to keV energies and to catch and cool them in a trap.

6. Summary

The measurement of the g-factor of the bound electron in hydrogenic ions promises interesting results in the field of bound-state QED. Today, experimental data are available only on atomic hydrogen and the helium ion ($^4He^+$). With state-of-the-art techniques of cooling, storing and detecting a single ion in a Penning trap, the measurements can be extended to heavier hydrogenic ions. The available theoretical calculations are applicable only to light hydrogenic ions, because in the case of heavy hydrogenic ions the uncalculated higher-order QED corrections have to be taken into account.

The authors are grateful to I. Lindgren, E. Lindroth, H. Persson and G. Soff for helpful and stimulating discussions.

REFERENCES

[1] G. Breit, *Nature* **122**, 649 (1928).
[2] H. Margenau, *Phys. Rev.* **57**, 383 (1940).
[3] T. Kinoshita, in: *Quantum Electrodynamics,* ed. by T. Kinoshita, World Scientific, Singapore 1990.
[4] H.G. Dehmelt, *Rev. Mod. Phys.* **62**, 525 (1990).
[5] H. Grotch, R.A. Hegstrom, *Phys. Rev.* **4**, 59 (1971); see also: R. Faustov, *Phys. Lett.* **33 B**, 422 (1970); F.E. Close, H. Osborn, *Phys. Lett.* **34 B**, 40 (1971).
[6] I. Lindgren, H. Persson, private communication, and G. Soff, private communication.

[7] I. Klaft *et al., Phys. Rev. Lett.* **73**, 2425 (1994).
[8] E. Lindroth, private communication.
[9] F.G. Walther, W.D. Phillips, D. Kleppner, *Phys. Rev. Lett.* **28**, 1159 (1972).
[10] J.S. Tiedeman, H.G. Robinson, *Phys. Rev. Lett.* **39**, 602 (1977).
[11] C.E. Johnson, H.G. Robinson, *Phys. Rev. Lett.* **45**, 250 (1980).
[12] L.S. Brown, G. Gabrielse, *Rev. Mod. Phys.* **58**, 233 (1986).
[13] G. Gabrielse *et al., Phys. Rev. Lett.* **65**, 1317 (1990).
[14] J. Arianer, A. Cabrespine, C. Goldstein, *Nucl. Instrum. Methods Phys. Res.* **193**, 401 (1982).
[15] W. Lötz, *Z. Phys.* **216**, 241 (1968).
[16] R.E. Marrs, S.R. Elliott, D.A. Knapp, *Phys. Rev. Lett.* **72**, 4082 (1994).
[17] R. Mann, *Z. Phys.* **D3**, 85 (1986).